



EXPERIMENTAL INVESTIGATION OF SLENDER PRESTRESSED BRICK WALLS

Edward M. Lacika¹, Robert G. Drysdale²

ABSTRACT

This paper reports on an investigation of the out-of-plane structural behaviour of slender prestressed (restrained tendon) brick walls. In particular, the interactions between slenderness, axial load, and prestress are discussed.

At all slenderness levels, the prestressed walls supported axial loads greater than those which would typically be found in low-rise construction. Also, the use of prestress was more effective at higher slenderness, and controlled the onset of cracking. At low slenderness, the axial load behaved as a prestress. The prestressed walls also exhibited a high resistance to repeated loading, which made it possible to perform multiple tests on each wall.

INTRODUCTION

Although prestressing offers significant structural and possibly economical benefits (Garrity et al., 1994) over conventional reinforcing, the lack of available details and design guidance for its application to masonry are deterrents from its widespread use. To the limited extent that prestressed masonry has been used, wall construction and the related research involved heavy duty wall systems, such as diaphragm walls used as retaining structures (Lacika, 1994). Consequently, there is a need to investigate the structural behavior of prestressed single wythe brick walls, so that the benefits of prestressing may be realized in lighter construction. Considering the slender nature of a single wythe brick wall, the study of slenderness effects is an essential feature of this research.

1 Engineer, Hamilton, Ontario, Canada

2 Professor, McMaster University, Hamilton, Ontario, Canada

EXPERIMENTAL DETAILS

Material Properties

The properties of the materials used in this investigation are listed in Table 1. All the masonry unit tests were conducted according to CAN3-A82.2. The walls were constructed with clay bricks, having five cylindrical cores with a 37 mm mean diameter. The dimensions of the bricks were found to be within allowable tolerances for bricks specified as being 90×90×290 mm. Type S mortar was used in the construction of the prisms and walls. The mortar tests were conducted according to CSA Standard A179M "Mortar and Grout for Unit Masonry". The standard used for testing compressive strength of masonry prisms was CSA A369.1, "Method of Test for Compressive Strength of Masonry Prisms". For guidance on construction of the specimens and testing of the flexural bond, the ASTM Standard C1072 was used. Twenty-six millimeter diameter prestressing bars ($A_s = 551 \text{ mm}^2$) were used in the construction of the walls. No laboratory tests were performed on the prestressing steel, instead the manufacturer's specifications were used.

Table 1 Material properties.

Material	Mean	COV (%)
Brick Compressive Strength (MPa)	gross area	70.5
	net area	109.7
Mortar Compressive Strength (MPa)	14.4	14.7
Masonry Compressive Strength f_m (MPa)	bedded area	43.2
	net area	32.0
Masonry Modulus of Elasticity E_m (MPa)	bedded area	16500
	net area	12200
Masonry Tensile Strength (MPa)	gross area	0.39
	net area	0.40
Prestressing Steel Minimum Ultimate Strength (MPa)	1030	N.A.
Prestressing Steel Modulus of Elasticity E_s (MPa)	200000	N.A.

Wall Specimens

A total of six prestressed wall specimens were constructed with a deformed prestressing bar (restrained) at the center of each wall cross-section. Bricks of 90 mm width were chosen so that very slender walls could be tested within the height limitations of the laboratory. Numerous factors were considered when choosing the reinforcement and the appropriate dimensions of the test walls. For efficient use of masonry, the bar size was chosen sufficiently large (26 mm diameter, $A_s=551 \text{ mm}^2$) to provide adequate prestressing force, without the need for frequent spacing of smaller diameter bars. A sufficient width of wall (1.2 m) was needed to ensure only out-of-plane behaviour and to provide an adequate area to resist prestressing. The lower limit on the height was taken to be the

maximum allowed by the standard "Masonry Design for Buildings" (CAN3-S304-M84), which is 2.7 m for a 90 mm thick wall. To ensure that the slenderness limit, in relation to capacity, was fully investigated, the tallest wall tested was 6 m, with a corresponding slenderness ratio (h/t) of 67. Data in the intermediate range was provided by a 4.2 m high wall ($h/t=47$). For practical reasons, the construction time, amount of materials needed, and handling of specimens were also considered in the sizing of the walls. The dimensions of the wall specimens are listed in Table 2.

Table 2 Wall dimensions.

Specimen Name	Width (m)	Height (m)	Slenderness (h/t)
w1	1.2	2.7	30
w3	1.2	2.7	30
w5	1.2	4.2	47
w6	1.2	4.2	47
w7	1.2	6.0	67
w8	1.2	6.0	67

Note: All walls were constructed using 90×90×290 mm bricks with 10 mm mortar joints.

After sufficient curing and prior to testing, each wall was prestressed to a desired level. As illustrated in Fig. 1, prestressing of the specimens was accomplished using a hydraulic jack. A coupler with an extension was screwed on the prestressing bar, and a prestressing chair and jack were fitted over the assembly. As the wall was stressed, the prestressing force was monitored by a load cell. When the wall was stressed to the desired level, the prestressing nut was tightened with a wrench, and then the jack was released. If, after the lock-off losses, the prestressing force was not sufficiently close to the required value, the procedure was repeated.

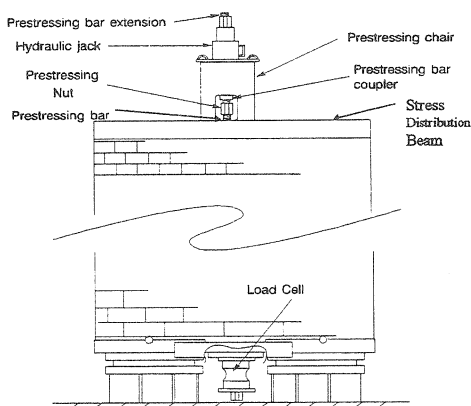


Fig. 1 Prestressing apparatus.

Test Apparatus

To test the walls, the reaction frame shown in Figs. 2 and 3 was constructed.

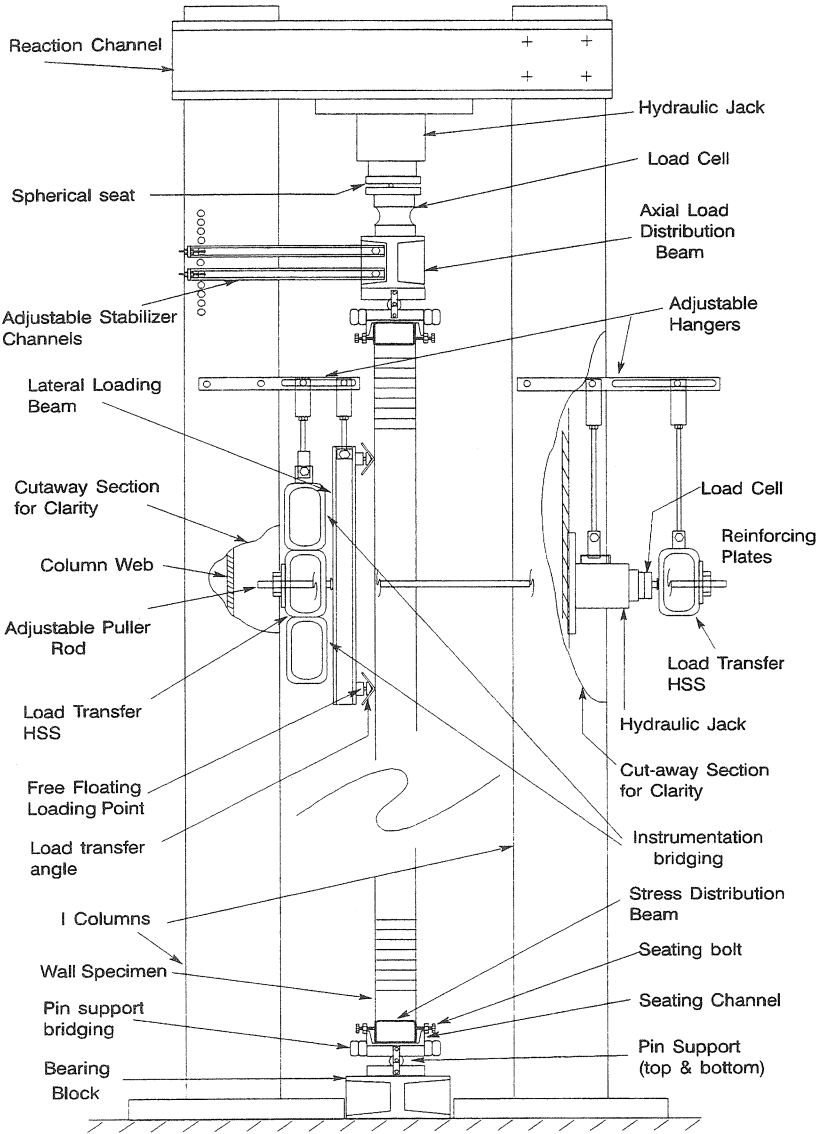


Fig. 2 End elevation of reaction frame and test set-up.

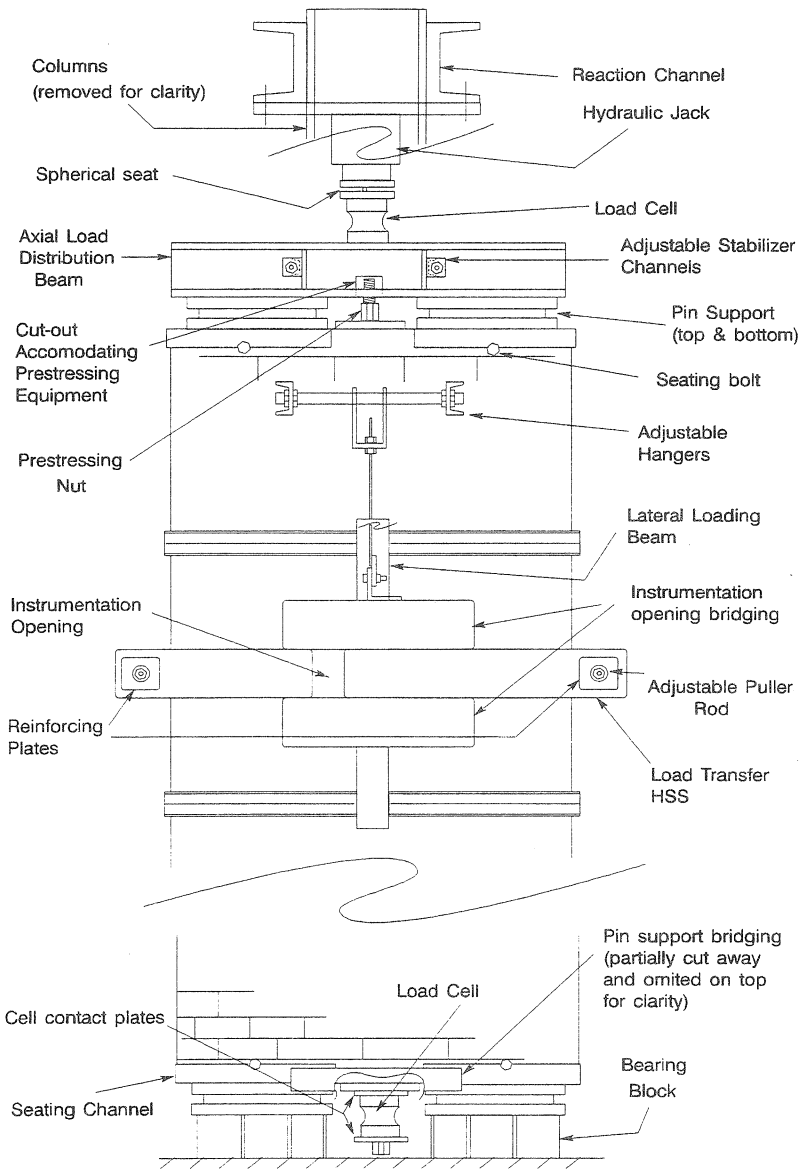


Fig. 3 Face elevation of the compression side of the test set-up and reaction frame.

As can be seen, the wall specimen was simply supported and the axial and lateral loads were applied using hydraulic jacks and load distribution beams. The lateral load was applied at $h/\sqrt{8}$ (h = height) from each end of the wall, while axial load was applied concentrically and maintained constant.

The axial, lateral, and prestress forces were measured by load cells and the deflections were monitored by seven LPDTs equally spaced along the height of the walls. Both forces and deflections were recorded by a data acquisition system. For more details see Lacika, 1994.

RESULTS AND DISCUSSION

Demonstrated in Figs. 4 to 6 are the influences of slenderness and axial load on responses of the prestressed walls. Primary moment (lateral load moment) versus deflection at mid-height is plotted for various axial loads and heights. In the legend, the first number after the "w" is the wall identification, and the second number is the amount of prestress force in terms of percent of ultimate strength of the prestressing bar (10 = 57 kN, 20 = 114 kN, 30 = 170 kN). The last number indicates the axial load in kN. The permanent set and construction imperfections are not shown but can be assumed to cause a decreased primary moment. If the values were used for design, a conservative and thus safe estimate of the primary moment resistance would be obtained. For ease of comparison, the axis scales and the curve markers for each axial load for a given slenderness are the same in all three figures.

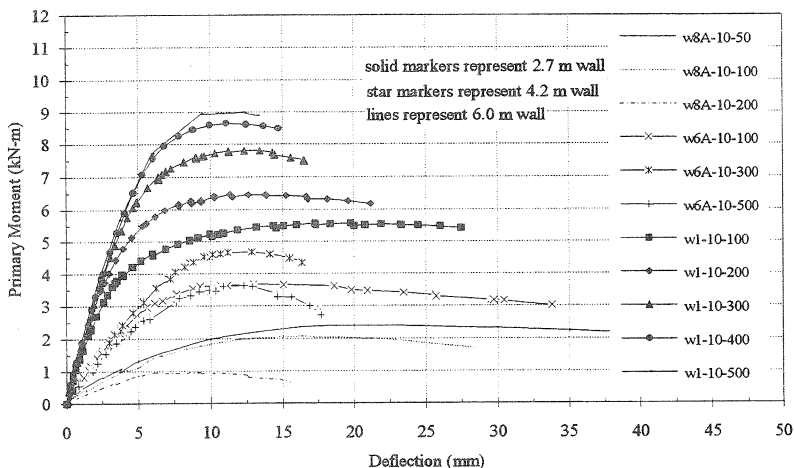


Fig. 4 Influence of slenderness and axial load at 57 kN prestress.

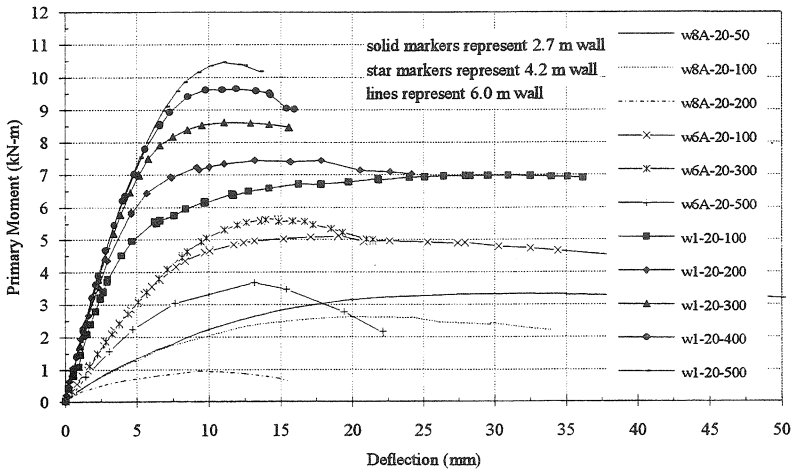


Fig. 5 Influence of slenderness and axial load at 114 kN prestress.

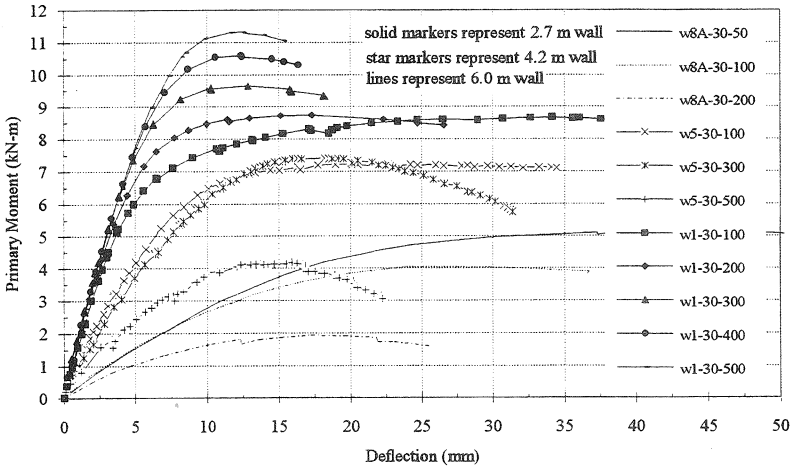


Fig. 6 Influence of slenderness and axial load at 170 kN prestress.

As can be seen, slenderness had a strong influence on behaviour. As the height of the walls increased, the increase in bending moment due to the P- Δ effect resulted in a decrease in the primary moment resistance. For example, in Fig. 5 at 300 kN axial load, the moment capacity decreased from 8.5 kN-m to 5.5 kN-m as the height was increased from 2.7 m (Wall 1) to 4.2 m (Wall 6A). The permanent sets of Wall 1 and Wall 6A were 3.9 and 4.1 mm, respectively, before application of the 300 kN axial load. Therefore, the eccentricities of axial loads were quite similar.

Depending on slenderness, axial load had either a positive or a negative effect on the primary moment resistance. For the 2.7 m wall, increases in axial load increased the primary moment resistance. For the 4.2 m wall, however, axial loads up to 300 kN increased the maximum value of the primary moment, whereas at 500 kN sizable decreases were observed. At the 6 m height all increases in axial loads resulted in decreased primary moment capacities.

Although axial load either increased or decreased the maximum primary moment capacity depending on slenderness, it can be seen from Figs. 4 to 6 that increases in prestress always increased capacity. Therefore, as was expected, prestress does not contribute to the secondary moment when the tendon is restrained (i.e. prevented from changing position in the cross-section as the wall deflects).

Table 3 is a summary of the maximum primary moments for several axial loads as the prestress was increased from 57 kN to 170 kN. Also shown in Table 3 are the

Table 3 Summary of the maximum primary moments for various heights.

Height (m)	Axial Load (kN)	Maximum primary moment, permanent set before application of load (kN-m, mm)		% Increase in maximum primary moment
		57 kN Prestress	170 kN Prestress	
2.7	100	5.7, 0	8.6, 0	51
	200	6.4, 2	8.8, 6	38
	300	7.8, 2	9.6, 7	23
	400	8.6, 2	10.6, 7	23
4.2	100	3.7, 3	7.2, 7	95
	200	4.5, 3	7.5, 8	67
	300	4.7, 4	7.5, 9	60
	400	4.5, 5	6.8, 11	51
6.0	50	2.5, 6	5.2, 11	108
	100	2.1, 8	4.1, 12	95
	200	0.9, 9	1.9, 12	111

permanent sets and the percent increases in the maximum primary moments corresponding to the increase in prestress. As can be seen, the percent increase in maximum primary moment increased with height. Except for the 6 m wall with axial load of 200 kN, the percent increase in maximum primary moment decreased with increased axial load. Thus, prestressing was more effective at greater slenderness, and less effective as axial load increased.

Since permanent set was always greater at the 170 kN prestress level, the increases in maximum primary moments with prestress are conservative and may be greater for undisturbed walls. Therefore, due to permanent set, the benefit of increase in prestress is underestimated.

The interaction between slenderness, axial force, and prestress is summarized in Fig. 7. The prestress force and the height of the wall are indicated for each curve.

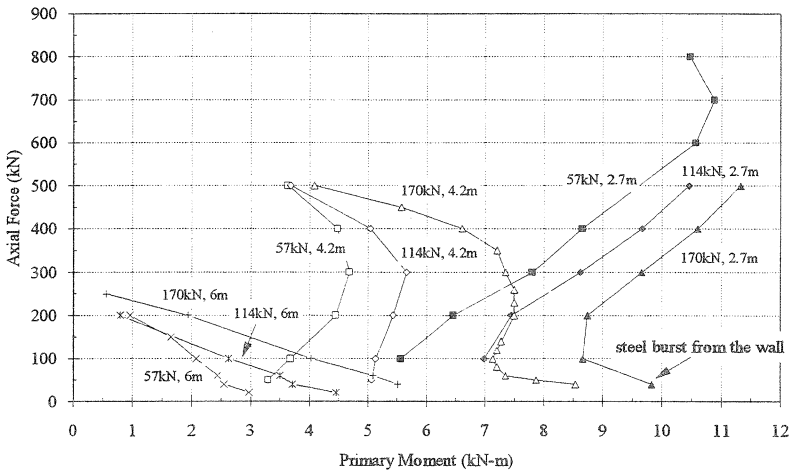


Fig. 7 Interaction between slenderness, axial load, and prestress.

For the prestress levels tested, it can be seen that slenderness is the most critical factor influencing the behaviour. With increased slenderness, the primary moment capacity decreased. Increases in prestress, however, increased the capacity and, to some extent, overcame some of the decrease caused by an increase in slenderness. This is most notable in the 4.2 m wall prestressed to 170 kN, where the capacity overlaps the 2.7 m wall prestressed to 57 kN. This overlap is also observed for the 6 m wall, prestressed to 170 kN, and the 4.2 m wall, prestressed to 57 kN. All walls failed by reaching a maximum primary moment, with the exception of Wall 3, which failed due to the prestressing bar bursting out of the wall.

A notable feature of the behaviour is demonstrated by inspecting the interaction diagram of the 4.2 m wall prestressed to 170 kN. For ease of discussion, the interaction curve for this wall is duplicated in Fig. 8.

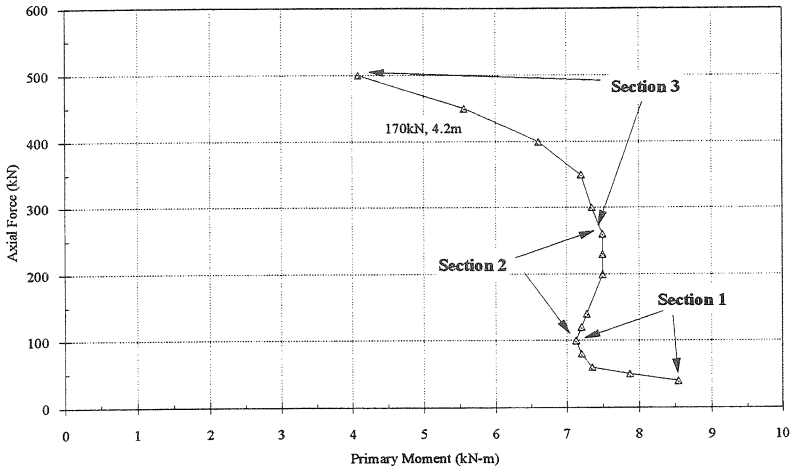


Fig. 8 Interaction diagram for a 4.2 m wall prestressed to 170 kN.

As can be seen, at axial loads less than 100 kN (Section 1 of the interaction diagram in Fig. 8), the primary moment decreased with increased axial load. For this range of axial loads, the greatest compressive strain in the masonry, including prestress and axial load, was 0.00111, which is approximately half of the strain corresponding to the maximum masonry stress. Thus, nonlinear material behaviour or material failure can be discounted as possible factors. The explanation for the unexpected behaviour of Section 1, however, can be obtained by inspection of Fig. 9. Illustrated in Fig. 9 is the primary moment and the corresponding deflection for the 4.2 m wall (Wall 5) prestressed to 170 kN and subjected to axial loads up to 100 kN. These experimental curves were used to construct Section 1 of the interaction diagram in Fig. 8. Because there was no more increase in the primary moment with deflection, the capacity had been reached. Although the axial loads are relatively small (compared to the axial capacity), in combination with the large deflections, the secondary moments are significant. For example, the 40 kN axial force and a 65 mm mid-height deflection creates a 2.6 kN-m secondary moment. This is equivalent to 30 % of the primary moment. Consequently, this and the discounting of the nonlinear material behaviour suggests that the decrease in moment with increased low axial load (Section 1 in Fig. 8) is caused by the P- Δ effect.

Because permanent set was present and contributed to the P- Δ effect, the possibility that permanent set could cause the decrease in capacity seen in Section 1 of Fig. 8 must be

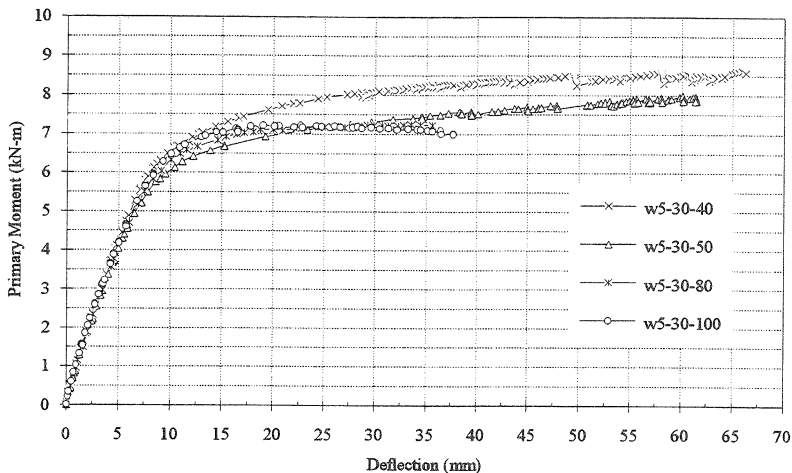


Fig. 9 Mid-height primary moment deflection, Wall 5, $h = 4.2$ m, prestress = 170 kN.

considered. However, this does not appear to be the case. If it is assumed that the decrease in Section 1 is caused by the permanent set being sufficiently large to control the $P-\Delta$ effect, then, as the testing proceeded with increases in axial load and permanent set accumulated, it would be expected that the primary moment would continue to decrease with increased axial load. This was not the case. For axial loads greater than 100 kN (Section 2 in Fig. 8), the trend of the interaction curve changed and an increase in the primary moment occurred. Consequently, permanent set could not have been the controlling factor in Section 1. This conclusion is further supported by the fact that the permanent set for axial loads in Section 1 (Fig. 8) did not exceed 15% of the total deflection and, hence, probably could not have been the controlling portion of the $P-\Delta$ effect.

The interaction curves for the 4.2 m and 2.7 m walls (Fig. 7) prestressed to 114 kN are not complete, but they also tend toward showing that, at relatively low axial loads, a decrease in primary moment can be expected with increased axial loads, as was more clearly shown at the 170 kN prestress, and for all levels of prestress for the 6.0 m walls. In the case of the 2.7 m wall prestressed to 170 kN, the failure at the lowest axial load shown in Fig. 7 was governed by a type of material failure (the prestressing bar burst out of the wall), but this does not alter the observation.

Sections 2 and 3 of the interaction diagram in Fig. 8 are also affected by the $P-\Delta$ effect. In Section 2, there is an increase in moment with increased axial force, and in Section 3 there is a decrease in moment with increase in axial load. Because of relatively high axial loads, permanent set is important in the behaviour in Section 3. For example, for the 4.2 m wall

prestressed to 170 kN, the primary moment capacity at 300 kN axial load was 7.4 kN-m. The corresponding total (primary + secondary) moment was 15.1 kN-m. Subtracting the primary moment from the total moment, gives a P- Δ moment of 7.7 kN-m. The mid-height moment due to the 9 mm permanent set is 2.7 kN-m, which is 35% of the P- Δ moment.

CONCLUSIONS

In summary, it was found that, except for Wall 3, the primary moment capacity was governed by the P- Δ effect. Increases in slenderness had the most dramatic impact on behaviour by decreasing the primary moment capacity and, depending on the magnitude, increased axial load either increased or decreased the capacity. At relatively low axial loads, however, there was an unexpected decrease in primary moment capacity with increased axial load due to the P- Δ effect. Increases in prestress always increased the capacity. This indicates that the restraint of the prestressing bar, keeping it in the center of the section, was sufficient to prevent the prestress force from noticeably contributing to the P- Δ effect.

REFERENCES

1. Garrity, S., and Nicholl, R., "Reinforced and Prestressed Masonry Earth Retaining Walls - A Cost Study", Proceedings of the 10th International Brick and Block Masonry Conference, Calgary, Alberta, Canada, July 5-7, 1994, pp.431-440
2. Lacika, E.M., Structural Investigation of Slender Prestressed Brick Walls, Master Thesis, Department of Civil Engineering, McMaster University, Hamilton, Canada, 1994, 176 pages
3. Shultz, A., and Scolforo, M., "An Overview of Prestressed Masonry", TMS Journal, August 1991, pp.6-21, Boulder, U.S.A.